Density functional theory study on biodiesel production from yeast lipid catalyzed by imidazolium ionic liquid

Yuwei Chen[a,b,d], Xiaolei Zhang[c], Yunwu Zheng[d], Jianchun Jiang[b], Feng Long[b], Wei Liu[a*], Junming Xu[b*], Xiaoan Nie[b*]

[a] School of Automotive Engineering, Jiangsu Provincial Key Laboratory of Eco-Environmental Materials, Yancheng Institute of Technology, Yancheng 224051, China

[b] Institute of Chemical Industry of Forest Products, Chinese Academy of Forestry, Nanjing 210042, China

[c] Department of Chemical and Process Engineering, University of Strathclyde, UK

[d] National Joint Engineering Research Center for Highly-Efficient Utilization Technology of Forest Biomass Resources, International Joint Research Center for Bioenergy, Southwest Forestry University, Kunming, 650224, PR China

[*] Corresponding authors: liuwei@ycit.edu.cn (W. Liu), xujunming@icifp.cn (J. Xu), niexiaoan@icifp.cn (X. Nie)

Abstract

Imidazolium ionic liquid is a novel and efficient catalyst for biodiesel production from oleaginous yeast. However, the catalytic mechanism of how imidazolium ionic liquid works in the reaction is not clear. Herein, Density functional theory (DFT) was employed to investigate the catalytic mechanism of three imidazolium ionic liquids in esterification and transesterification reactions. Pathways containing three intermediates and two transition states were proposed for the two reactions. In the subsequent DFT calculation, PBE0-D3BJ functional and 6-31G* basis set were used to optimize the intermediates and transition states. Then the Gibbs free energy of the intermediates and transition states in each reaction step was calculated to obtain the energy barrier for each reaction. The calculation results showed that 1-butyl-3-methylimidazolium hydrogen sulfate ([Bmim][HSO_4]) had the minimum energy barrier of 37.77 kcal/mol in esterification, and 1-sulfobutyl-3-methylimidazolium hydrosulfate ([HSO_3-Bmim][HSO_4]) had the minimum energy barrier of 20.80 kcal/mol in transesterification, which were consistent with previous experimental results. The catalytic mechanism validated in this study provides a new idea for subsequent optimization of imidazolium ionic liquid structure to improve their catalytic efficiency in biodiesel production from oleaginous yeast.

This is a peer-reviewed, accepted author manuscript of the following article: Chen, Y., Zhang, X., Zheng, Y., Jiang, J., Long, F., Liu, W., Xu, J., & Nie, X. (2023). Density functional theory study on biodiesel production from yeast lipid catalyzed by imidazolium ionic liquid. Journal of Molecular Liquids, 385, [122226]. https://doi.org/10.1016/j.molliq.2023.122226

Key words

Biodiesel, yeast lipid, imidazolium ionic liquid, DFT calculations

1.Introduction

Energy consumption and environment protection are two hot issues in recent decades[1, 2]. The fast population explosion, continuous industrialization and irreversible metropolitan expansion consumes fossil fuels excessively[3, 4]. To deal with the drawbacks of excessive use of fossil, China has taken the lead in promising of “peak carbon dioxide emissions” and “carbon neutral”[5]. In order to achieve the goals, the renewable biodiesel is a promising candidate to replace fossil fuels[6, 7]. Biodiesel (long-chain monoalkyl fatty acid esters) has many sources, such as agricultural wastes, waste cooking oil and non-edible oils[8, 9]. In recent years, oleaginous yeast has been a new kind source of biodiesel, for it has advantages of high lipid content, wide varieties of substrates and short cultivation cycles[10, 11]. Among all the oleaginous yeast, *Rhodosporidium toruloides* (*R. toruloides*) is a bright candidate. *R. toruloides* can accumulate more than 70% lipid in dry cells[12]. The lipid from *R. toruloides* consist of triacylglycerol (TAG), fatty acid (FFA), diacylglycerol (DAG) and monoacylglycerol (MAG)[13]. Because of these properties, *R. toruloides* is suitable for biodiesel production. In previous work, hydrothermal liquefaction showed to be a novel method to disrupt cell wall of *R. toruloides* and extract the lipid from the yeast[14].

In order to obtain biodiesel, the lipid extracted from *R. toruloides* needs to take transesterification or esterification reactions with methanol in the presence of catalyst. As there exists considerable fatty acid in the lipid, acid catalyst is suitable for the reaction in order to obtain biodiesel in one step. Sulfuric acid or p-Toluenesulfonic acid is often used as catalyst in the reactions. However, both of these acids are strong acids and they can be corrosive to equipment. Besides, the catalyst can not be recycled. Considering these drawbacks of traditional catalyst, acidic ionic liquid was introduced in converting yeast lipid to biodiesel[15-17]. In previous study, acidic ionic liquid

showed the similar catalytic effect with the strong acid, and they can be recycled with proper processes[18]. Hu et al. used acidic ionic liquid 1-sulfobutyl-3-methylimidazolium hydrosulfate ([HSO_3-Bmim][HSO_4]) as catalyst to convert waste oils containing 72% of free fatty acids to biodiesel, the yield of biodiesel achieved as high as 94.9% at the optimum conditions. Besides, the catalytic activity of the ionic liquid [HSO_3-Bmim][HSO_4] remained around 97% after re-use of 5 times[19]. Sun et al. used 1-butyl-3-methylimidazolium hydrogen sulfate ([Bmim][HSO_4]) as a solvent and acid catalyst for in-situ extractive transesterification of wet *Nannochloropsis* with methanol, the results showed that at optimum conditions, the biodiesel yield achieved as high as 95.28%, and the catalytic efficiency remained as 81.23% after the ionic liquid [Bmim][HSO_4] recycled 4 times. In previous work, [Bmim][HSO_4], [HSO_3-Bmim][HSO_4] and 1-butyl-3-methylimidazolium dihydrogen phosphate ([Bmim][H_2PO_4]) were used as catalysts in model compound experiments, which were designed to identify the catalytic effect of three AILs in biodiesel production.[8] The results showed [Bmim][HSO_4] had better catalytic effects on esterification reaction and [HSO_3-BMim][HSO_4] had better catalytic effects on transesterification reaction. The research only gave the experimental results, further investigation on the interaction between catalysts and reactant weren't discussed. The catalytic processes were also not inferred. So the reason why the specific catalyst has the best or worst catalytic effect was not clear.

Density functional theory (DFT) is a reliable method in studying the mechanisms and kinetics of reactions. Many catalytic processes involved ionic liquid have been investigated by DFT[20, 21]. Silva et al. used DFT to study the solvent effects on the acid-catalyzed ethanolysis of butyric acid monoglyceride[22]. It was found that the reaction proceeded through a concerted mechanism with a single transition state without the formation of a tetrahedral intermediate. Ma et al. used DFT to calculate the effects of hydrogen bond between three ionic liquids and cellulose before the transesterification of algae lipid[23]. However, the most calculations only primarily

focused on the solvent effect of ionic liquids, the catalytic effect and the catalytic process were not investigated. Li et al. used DFT to investigate a three-step transesterification catalyzed by a pyridinium-based Brønsted acidic ionic liquid[24]. The results showed that hydrogen bond was exited throughout the process. Based on this founding, the catalytic mechanism involving hydrogen bond was established. To best of our knowledge, the catalytic mechanism of esterification or transesterification by acid imidazolium ionic liquid [Bmim][HSO_4], [HSO_3-Bmim][HSO_4] and [Bmim][H_2PO_4] hasn't been studied.

In this work, the plausible mechanism of esterification and transesterification catalyzed by [Bmim][HSO_4], [HSO_3-Bmim][HSO_4] and [Bmim][H_2PO_4] was proposed. Based on the mechanism, the reaction processes were then designed. The structures of reactant, intermediate (IM) and products were optimized before the transition states (TS) were obtained. After all the basic work was completed, the energy barriers of each reaction catalyzed by three different acidic ionic liquids were obtained. As a result, the catalytic effects of the three different acidic ionic liquids were obtained eight. In comparison with the previous experiments results, the correction of the DFT calculation was validated. The validated catalytic mechanism will provide a new idea for subsequent optimization of imidazolium ionic liquid structure to improve their catalytic efficiency in biodiesel production from oleaginous yeast.

2.Methods

All calculations have been performed using the DFT method implemented in the commercial Gaussian 16 program package[25]. Molecular geometries of the model complexes were optimized applying the PBE0-D3BJ functional[26, 27]. For all atoms the 6-31G* basis set was used. As soon as the convergences of optimizations were obtained, the frequency calculations at the same level have been performed to identify all the stationary points as minima or transition states, which has the unique imaginary frequencies. The intrinsic reaction coordinate (IRC) calculations have been carried out to confirm that the transition structures can indeed connect the related reactant and

product[28]. All of the optimized geometries mentioned were built by GaussView 6.0[29].

The main component of fatty acid in yeast lipid was oleic acid, which accounted about half in the lipid[14]. Synthetically considering the calculation accuracy and efficiency, the reactant of fatty acid in esterification was modelled as 4-Hexenoic acid with a linear carbon chain length of six carbon atoms containing an ethylenic bond ($CH_3CH=CHCH_2CH_2COOH$), and the monoacylglycerol was modelled as 2,3-dihydroxypropyl (4E)-hexenoate ($CH_3CH=CHCH_2CH_2COOCHOHCH_2OH$).

3.Results and discussion

With the functional and the basis set, the molecular geometries of the three acidic ionic liquid were firstly optimized. The results are shown in Fig. 1.

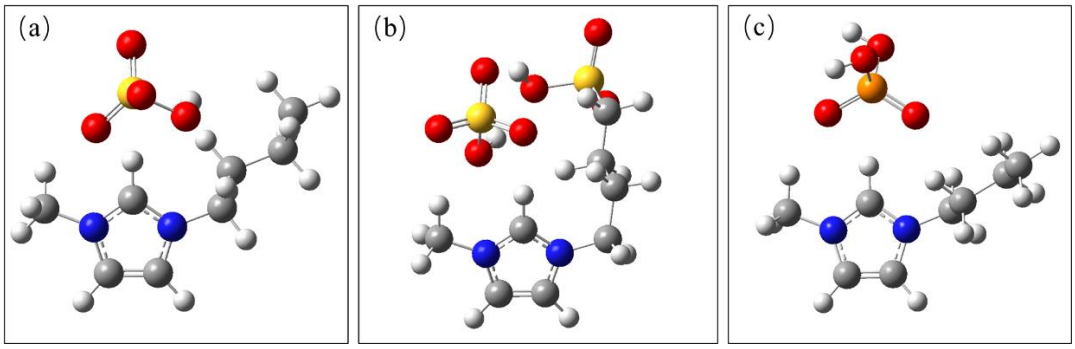

Fig. 1. Molecular Geometries of three acidic ionic liquid

（a）[Bmim][HSO_4] （b）[HSO_3-Bmim][HSO_4] （c）[Bmim][H_2PO_4]

3.1 Esterification

3.1.1 Reaction pathway

Taking other acidic ionic liquid catalyzed reaction pathways as reference[30], the reaction pathway of esterification catalyzed by [Bmim][HSO_4], [HSO_3-Bmim][HSO_4] and [Bmim][H_2PO_4] was proposed. Taking [Bmim][HSO_4] as the catalyst as example, the reaction pathway of esterification is shown in Fig. 2.

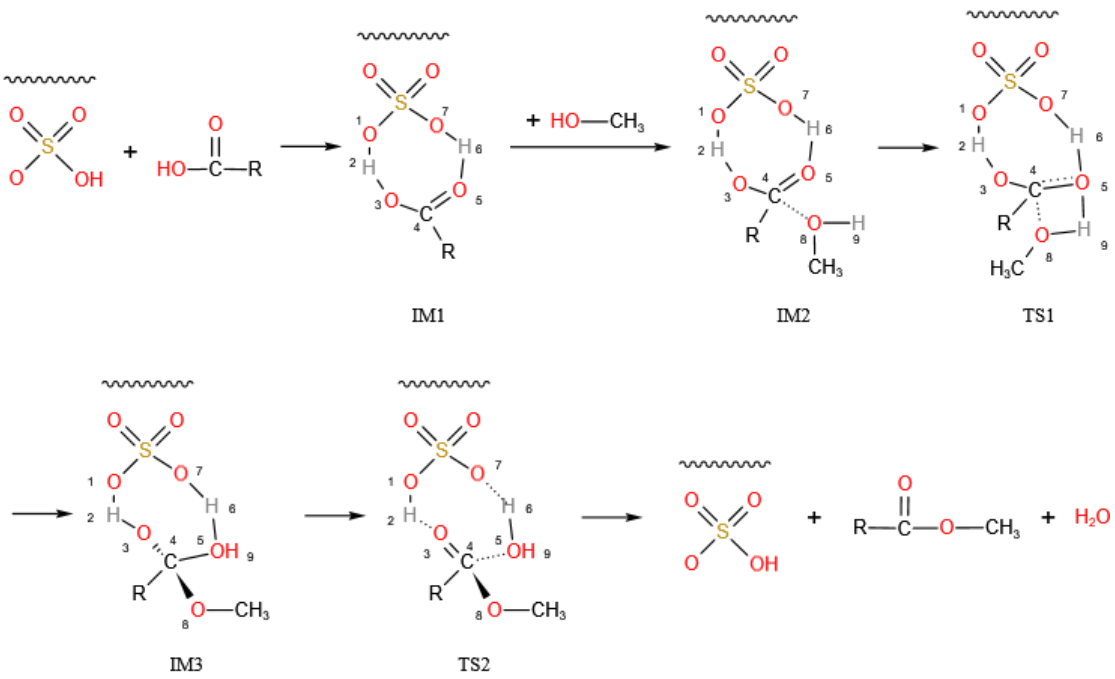

Fig. 2. Reaction pathway of esterification catalyzed by [Bmim][HSO_4]

As Fig. 2 shows, the total reaction contains two transition states (TS) and three intermediates (IM). Firstly, the acidic ionic liquid has effect on the FFA, and the carbonylic moiety of FFA was protonated, and it was activated to form IM1. Then the carbon atom (C4, the number means the number besides the atom in Fig. 2) of activated carbonyl combines with the oxygen (O8) of methanol and forms IM2. Due to the attraction between the hydrogen (H9) of hydroxyl from methanol and the oxygen (O5) of carbonyl from FFA, the bond between the two atoms establishes and thus IM2 transforms to TS1. TS1 is not stable, the oxygen (O5) of carbonyl from FFA has more attraction than the oxygen (O8) from methanol, so the hydrogen atom (H9) removes closely to the oxygen (O5) of carbonyl from FFA and forms hydroxyl. Due to the formation of hydroxyl, the attraction between the carbon atom (C4) and the oxygen atom (O5) from carbonyl decreases, so the double bond between the two atoms is broken and it becomes a single bond, so a tetrahedral structure is formed with the transformation of TS1 to IM3. With the increasing departure of the oxygen atom (O5) from the carbon atom (C4), the attraction between the two atoms decreases, and the single bond between the two atoms becomes an imaginary bond. Due to the attraction between the oxygen atom (O5) and the hydrogen atom (H6) from acidic ionic liquid

increases, so the single bond between the hydrogen atom (H6) and the oxygen atom (O7) from the acidic ionic liquid becomes an imaginary bond. At the same time, the attraction between the carbon atom (C4) and the oxygen atom (O3) increases, so the single bond between the two atoms becomes a double bond. The attraction between the hydrogen atom (H2) and oxygen atom (O3) of hydroxyl from FFA decreases, the single bond between the two atoms becomes an imaginary bond. The process is the transformation of IM3 to TS2. After the TS2 forms, all the imaginary bonds breaks, thus the fatty acid methyl ester and water forms. The reaction pathways catalyzed by the other two acidic catalytic liquid [HSO_3-Bmim][HSO_4] and [Bmim][H_2PO_4] are the same with that catalyzed by [Bmim][HSO_4].

3.1.2 Optimization of IMs and TSs

Based on the reaction pathway above, the structures of IMs and TSs in esterification catalyzed by [Bmim][HSO_4], [HSO_3-Bmim][HSO_4] and [Bmim][H_2PO_4] were optimized. The results are shown in Fig. 3, Fig. 4 and Fig. 5. As Fig. 3 shows, in IM1, there exists hydrogen bond between the oxygen atom (O33) of carbonyl from FFA and the hydrogen atom (H26) from the acidic ionic liquid, there also exists hydrogen bond between the oxygen atom (O23) from ionic liquid and the hydrogen atom (H35). The bond lengths of hydrogen bonds are 1.677Å and 1.597Å respectively, and the bond orders are both 0.1. The results reveal that these hydrogen bonds are weak. In IM2, when methanol participates in the reaction, there exists hydrogen bond between the hydrogen atom (H54) of hydroxyl from methanol and the oxygen (O23) from the ionic liquid, the bond length is 1.900Å, and the bond order is 0.1, indicating that the hydrogen bond is weak. Due to the influence of hydrogen atom (H54), the bond length between H35 and O23 increases to 1.662Å, at the same time, the bond length between H26 and O33 decreases to 1.528Å. The results show the distance between H26 and O33 is decreasing, the interaction between the two atoms is strengthening.

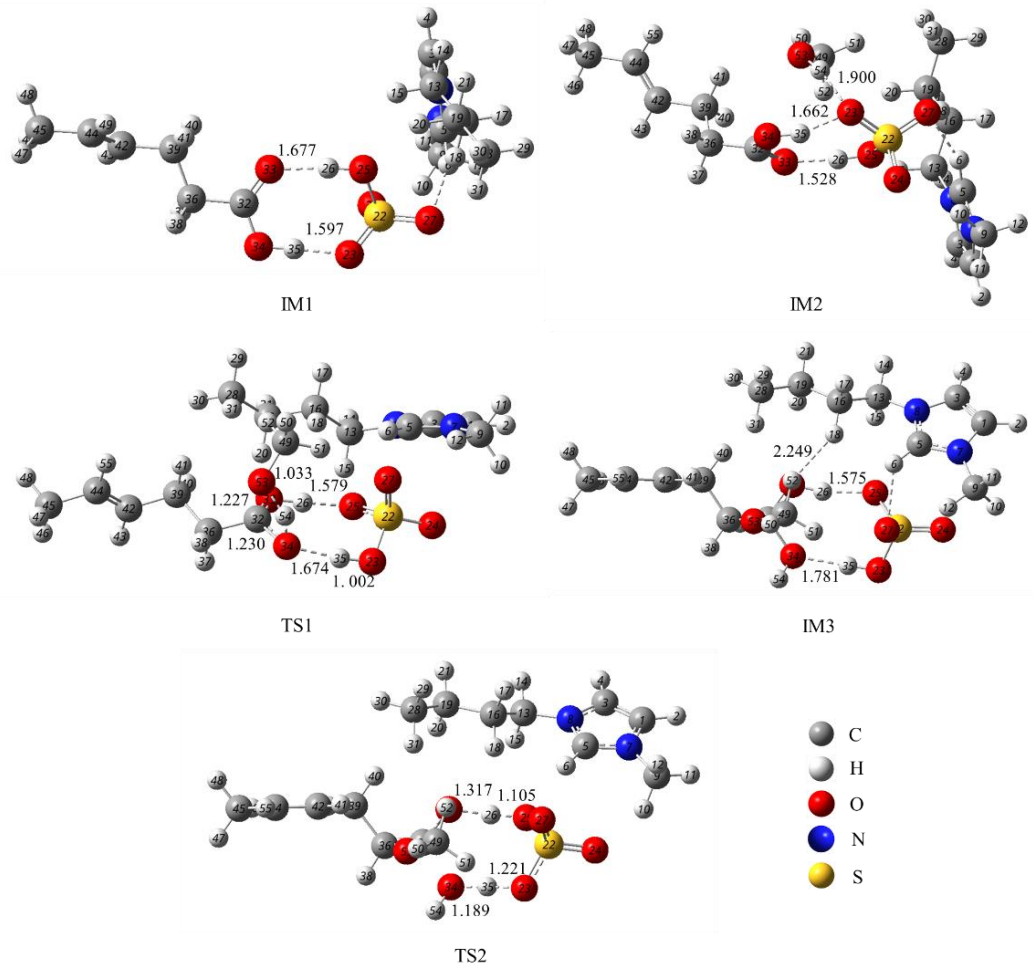

Fig. 3 IMs and TSs in esterification catalyzed by [Bmim][HSO_4]

In TS1, the bond length between H26 and O23 decreases to 1.013Å and the bond order increases to 1.0, this means there has formed a stable bond between the hydrogen atom H26 and oxygen atom O33. There is a hydrogen bond between H54 and O34, the bond length is 1.230Å and the bond order is 0.5, which means the hydrogen bond is forming but it is not stable enough. At the same time, the bond between O53 and C32 is forming, the bond length is 1.401Å and the bond order is 1.0, the results demonstrate that the tetrahedral structure has established. After the geometry of TS1 was optimized, an imaginary frequency of 1597.38 icm^{-1} was obtained. The frequency is corresponding with vibration of the movement of H54 from O53 to O34. In IM3, the hydrogen bond between H54 and O53 disappears, while there forms a bond between H54 and O34, the bond length and bond order are 0.968Å and 1.0 respectively, which means the bond between H54 and O34 is stable. The length of hydrogen bond between H35 and O33 is

196 1.781 Å, and the bond order is 0.1. The length of hydrogen bond between H26 and O25
197 is 1.575 Å, and the bond order is 0.1. The results indicate the two hydrogen bonds are
198 weak. In TS2, the bond between O34 and C32 breaks. The bond length between H35
199 and O34 decreases to 1.189 Å, and the bond order is 0.5. The bond length between H35
200 and O21 increases to 1.221 Å, and the bond order is 0.5. These phenomena demonstrate
201 that the H35 has a tendency of transferring from O21 to O34. At the same time, the
202 bond length between H26 and O25 decreases to 1.105 Å, and the bond length between
203 H26 and O33 increases to 1.317 Å. This indicates that H26 has a tendency of
204 transferring from O33 to O25. When the TS2 is optimized, an imaginary frequency of
205 873.96 icm^{-1} is obtained. The frequency is corresponding with vibration of the
206 movement of H35 from O21 to O34, H26 from O33 to O25 and the departure of O34
207 from C32. The vibration is exactly the generation path of fatty acid methyl ester and
208 water.

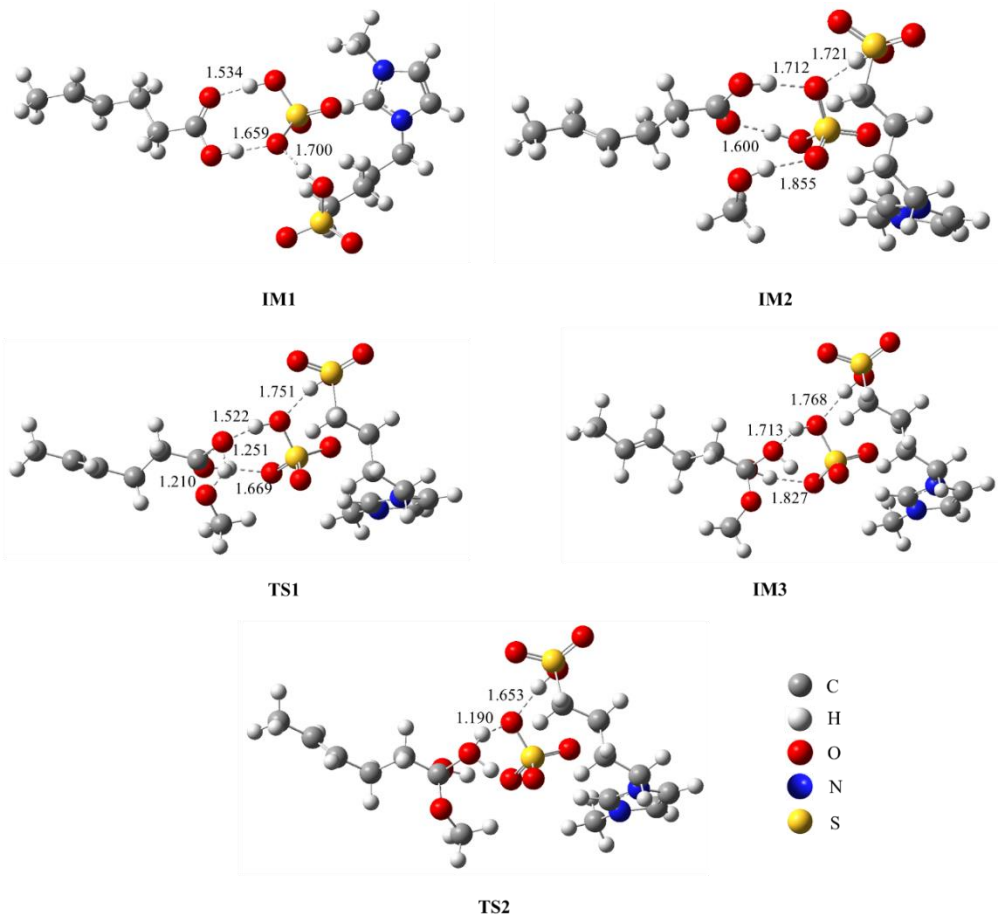

209

210 Fig. 4 IMs and TSs in esterification catalyzed by [HSO_3-Bmim][HSO_4]

211 Fig. 4 and Fig. 5 are the structures of IMs and TSs in esterification catalyzed by [HSO_3-
212 Bmim][HSO_4] and [Bmim][H_2PO_4]. The reaction processes are similar with that
213 catalyzed by [Bmim][HSO_4]. The imaginary frequency of TS1 and TS2 catalyzed by
214 the three ionic liquids is shown in Table 1.

215 Table 1 Imaginary frequency of TS1 and TS2 catalyzed by the three ionic liquids (icm^{-1})

	[Bmim][HSO_4]	[HSO_3-Bmim][HSO_4]	[Bmim][H_2PO_4]
TS1	1597.38	1579.39	1591.98
TS2	873.96	201.35	616.80

216

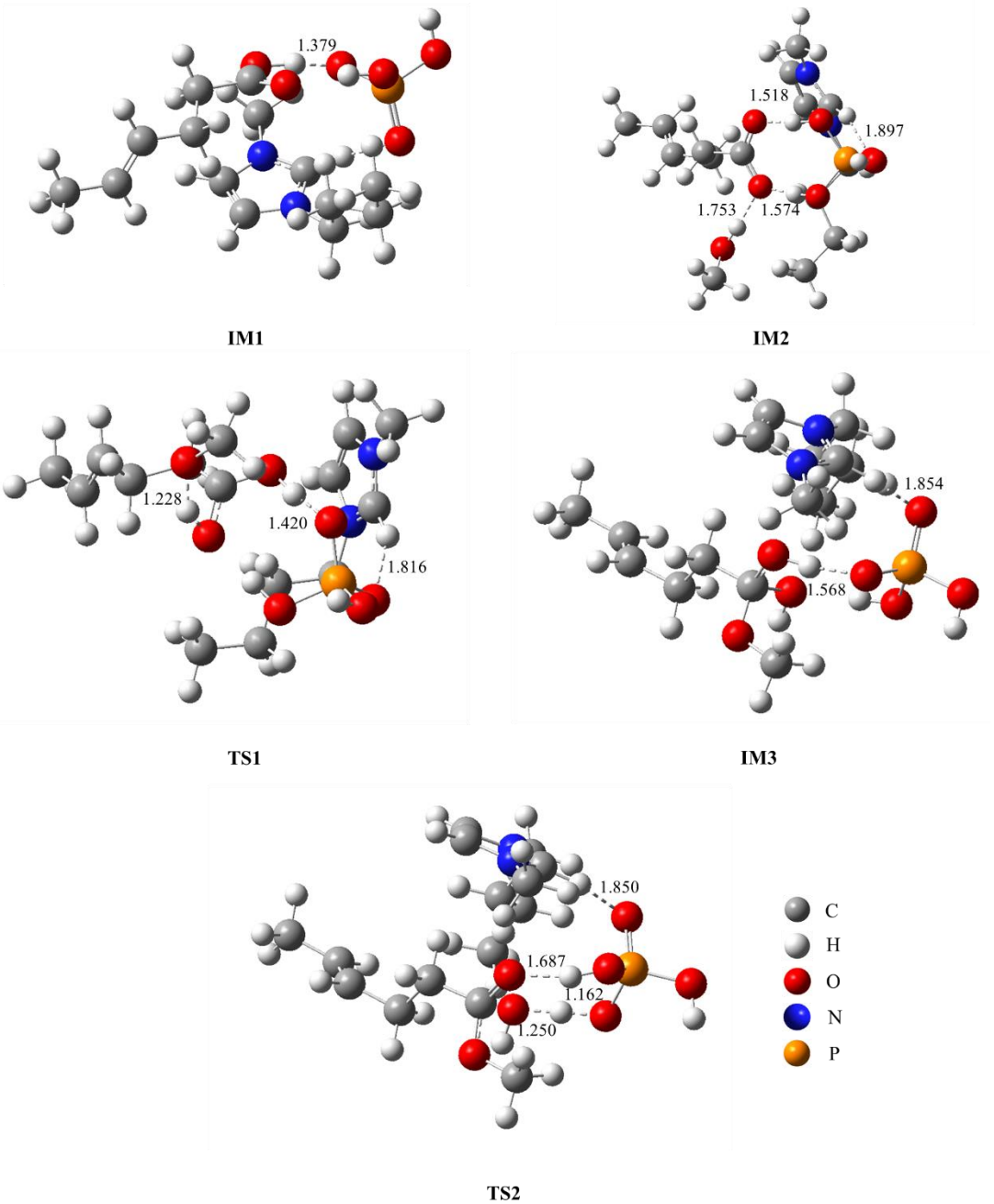

217

Fig. 5 IMs and TSs in esterification catalyzed by [Bmim][H_2PO_4]

3.1.3 Analysis of Gibbs free energy

After all the geometry of IMs and TSs was optimized, the frequency of each IMs and TSs was calculated. Then the Gibbs free energy was obtained. The results are shown in Table 2.

Table 2 Gibbs free energy of each phase in esterification catalyzed by three ionic liquids (Hartree)

	[Bmim][HSO_4]	[HSO_3-Bmim][HSO_4]	[Bmim][H_2PO_4]
R1	-384.56	-384.56	-384.56
R2	-115.55	-115.55	-115.55
Ionic Liquid	-1121.88	-1745.32	-1065.78
IM1	-1506.45	-2129.89	-1450.36
IM2	-1622.00	-2245.44	-1565.92
TS1	-1621.94	-2245.38	-1565.85
IM3	-1621.98	-2245.42	-1565.89
TS2	-1621.96	-2245.40	-1565.88
Product	-423.79	-423.79	-423.79
H_2O	-76.32	-76.32	-76.32

R1: $CH_3CH=CHCH_2CH_2COOH$

R2: CH_3OH

Product: CH_3-CH=CH-CH_2-CH_2-$COOCH_3$

Based on the calculation results in Table 2, taking the Gibbs free energy of ionic liquid as zero, then calculate the difference of the Gibbs free energy (ΔG) of each IMs and TSs relative to ionic liquid. The calculation results are shown in Fig. 6. From Fig. 6, it is easy to obtain the energy barrier (ΔG_{max}) in the esterification reactions catalyzed by different ionic liquids. By comparing the difference of ΔG_{max}, the reason why the three ionic liquids have different catalytic effects can be easily concluded.

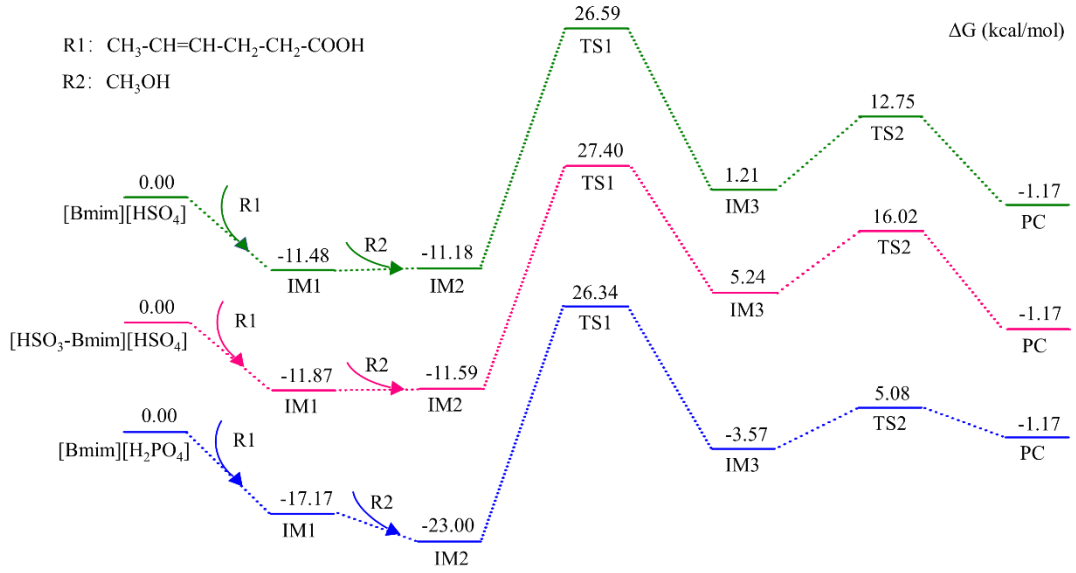

Fig. 6 Gibbs free energy in each phase of esterification catalyzed by three ionic liquids

In Fig. 6, it is obvious IM1 is a combination of ionic liquid and fatty acid, and IM2 is the combination of all reactant and catalyst, so the reactions begin from IM2. According to rate-limiting step theory suggested by Murdoch[31], the reaction can be divided into one period, i.e., from the ionic liquid to PC. The reaction contains two energy barriers, which are from IM2 to TS1 and IM3 to TS2 respectively. It is not difficult to be concluded that the energy barrier of IM2 to TS1 is higher than that of IM3 to TS2. So the rate-limiting step is IM2 to TS1. The ΔG_{max} of esterification catalyzed by [Bmim][HSO_4], [HSO_3-Bmim][HSO_4] and [Bmim][H_2PO_4] are 37.77 kcal/mol, 38.99 kcal/mol and 49.34 kcal/mol, respectively. The results demonstrate that the ΔG_{max} of esterification catalyzed by [Bmim][HSO_4] is the lowest, and [Bmim][H_2PO_4] is the highest. And of course [Bmim][HSO_4] and [Bmim][H_2PO_4] had the best and the worst catalytic effects respectively. The DFT results are consistent with the experimental results[8].

3.2 Transesterification

3.2.1 Reaction pathway

Taking transesterification pathway catalyzed by pyridinium based ionic liquid as reference[24, 32], the reaction pathway catalyzed by [Bmim][HSO_4], [HSO_3-

Bmim][HSO_4] and [Bmim][H_2PO_4] was proposed. Taking [Bmim][HSO_4] as the catalyst as example, the reaction pathway of transesterification is shown in Fig. 7.

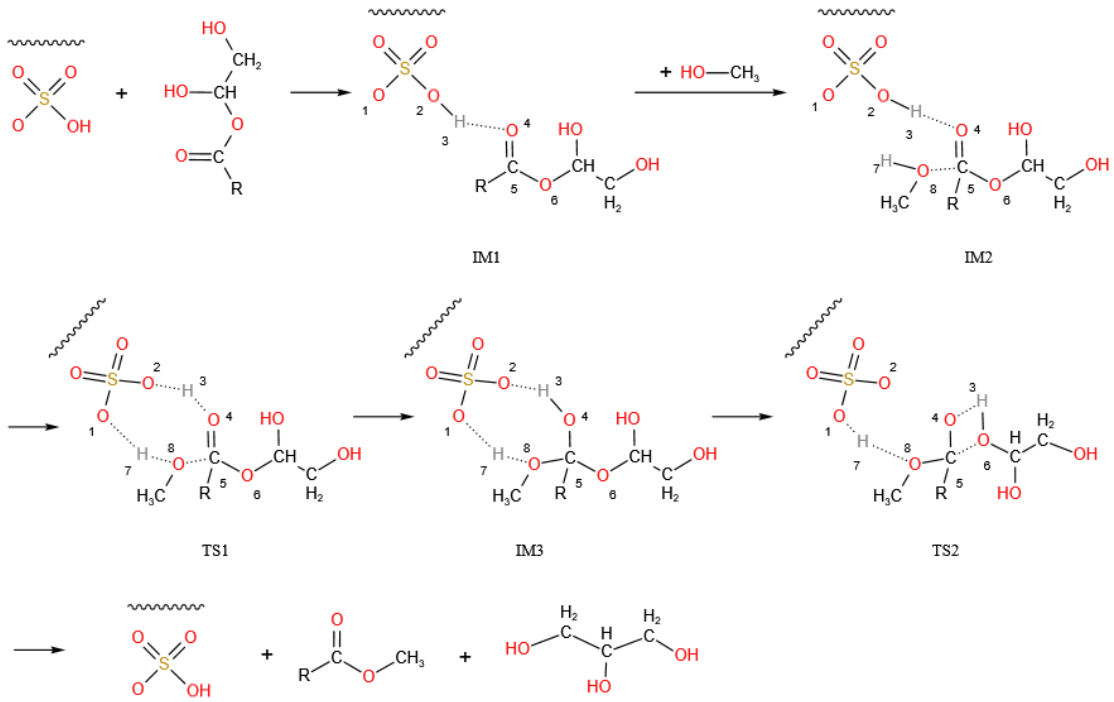

Fig. 7 Reaction pathway of transesterification catalyzed by [Bmim][HSO_4]

In Fig. 7, the hydrogen atom (H3) from [Bmim][HSO_4] was attracted by the oxygen atom (O4) of carbonyl from MAG, and a hydrogen bond is formed between the two atoms. This process is also the formation of IM1. After the combination of IM1 with methanol, the carbon atom (C5) from carbonyl has attraction on the oxygen atom (O8) of methanol, and an imaginary bond is formed between the two atoms. During this process, IM2 is also formed. As there exists attraction between the oxygen atom (O1) of the ionic liquid and the hydrogen atom (H7) of methanol, a hydrogen bond is formed between the two atoms. During this process, IM2 transforms to TS1. After TS1 is formed, the attraction between the oxygen atom (O1) and hydrogen atom (H7) is strengthened, the hydrogen atom (H7) has the trend of movement from O8 to O1, so the bond between the hydrogen atom (H7) and the oxygen atom (O8) becomes an imaginary bond. At the same time, the attraction between the oxygen atom (O4) and hydrogen atom (H3) is strengthened, the hydrogen atom (H3) has the trend of movement from O2 to O4, so the bond between the hydrogen atom (H3) and the oxygen atom (O2) becomes an imaginary bond. With the continuous movement of hydrogen

atom (H3) from O2 to O4, the interaction between H3 and O4 becomes stronger, which makes the interaction between O4 and C5 becomes weaker, so the double bond between O4 and C5 becomes a single bond. As a result, the interaction between C5 and O8 becomes stronger, so the imaginary bond between the two atoms becomes a single bond. These processes lead the transformation of the structure from TS1 to IM3, and the tetrahedral structure centered on carbon atom (C5) is also formed. With the movement of hydrogen atom (H3) in space, the atom H3 has interaction with the oxygen atom (O8), and there exists a hydrogen bond between the two atoms. This is also the transformation of IM3 to TS2. Due to the attraction of O6 is strengthened, the interaction between O2 and H3 is disappeared, and the bond between the two atoms is broken. Besides, the bond between H3 and O4 becomes an imaginary bond. At the same time, the bond between O6 and C5 becomes an imaginary bond. After the imaginary bonds are broken in TS2, the fatty acid methyl ester and glycerol are produced. The reaction pathway catalyzed by the other two ionic liquid [HSO_3-Bmim][HSO_4] and [Bmim][H_2PO_4] is similar with that of [Bmim][HSO_4].

3.2.2 Optimization of IMs and TSs

Based on the reaction pathway above, the structures of IMs and TSs in transesterification catalyzed by [Bmim][HSO_4], [HSO_3-Bmim][HSO_4] and [Bmim][H_2PO_4] were optimized. The results are shown in Fig. 8, Fig. 9 and Fig. 10. As Fig. 8 shows, in IM1, there exists a hydrogen bond between the hydrogen atom (H31) from the ionic liquid and oxygen atom (O29) of carbonyl from MAG. The bond length of hydrogen bonds is 1.773Å, and the bond order is 0.1. The results reveal that the hydrogen bond is weak. In IM2, after the methanol participates in the action, a hydrogen bond appears between the hydrogen atom (H26) from methanol and the oxygen atom (O25) from the ionic liquid. The bond length is 1.877 Å, and the bond order is 0.5, which means the bond is weak. Due to the influence of methanol, the hydrogen bond between H31 and O29 decrease to 1.748 Å, and the bond order increases to 0.5. The phenomenon shows that the distance between H31 and O29 is shorten, and the

297 interaction between the two atoms is strengthening.
298 After the geometry changes to TS1, the length of hydrogen bond between H31 and O29
299 decreases to 1.375 Å, and the bond order is 0.5. The length of bond between H31 and
300 O23 increases from 0.995 Å to 1.093 Å. The phenomena demonstrate the hydrogen
301 atom H31 is transforming from O23 to O29, but the hydrogen bond between H31 and
302 O29 is not strong enough. Apart from this, the length of hydrogen bond between H26
303 and O25 decreases to 1.591 Å, and the bond between H26 and O49 increases from
304 0.995 Å to 1.012 Å. The bond orders of the two bonds are 1.0 and 0.5 respectively. This
305 indicates the hydrogen atom H26 is transforming from O49 to O25. After the geometry
306 of TS1 was optimized, a frequency of 238.68 icm^{-1} was obtained. The frequency is
307 corresponding with vibration of the movement of H31 from O23 to O29.

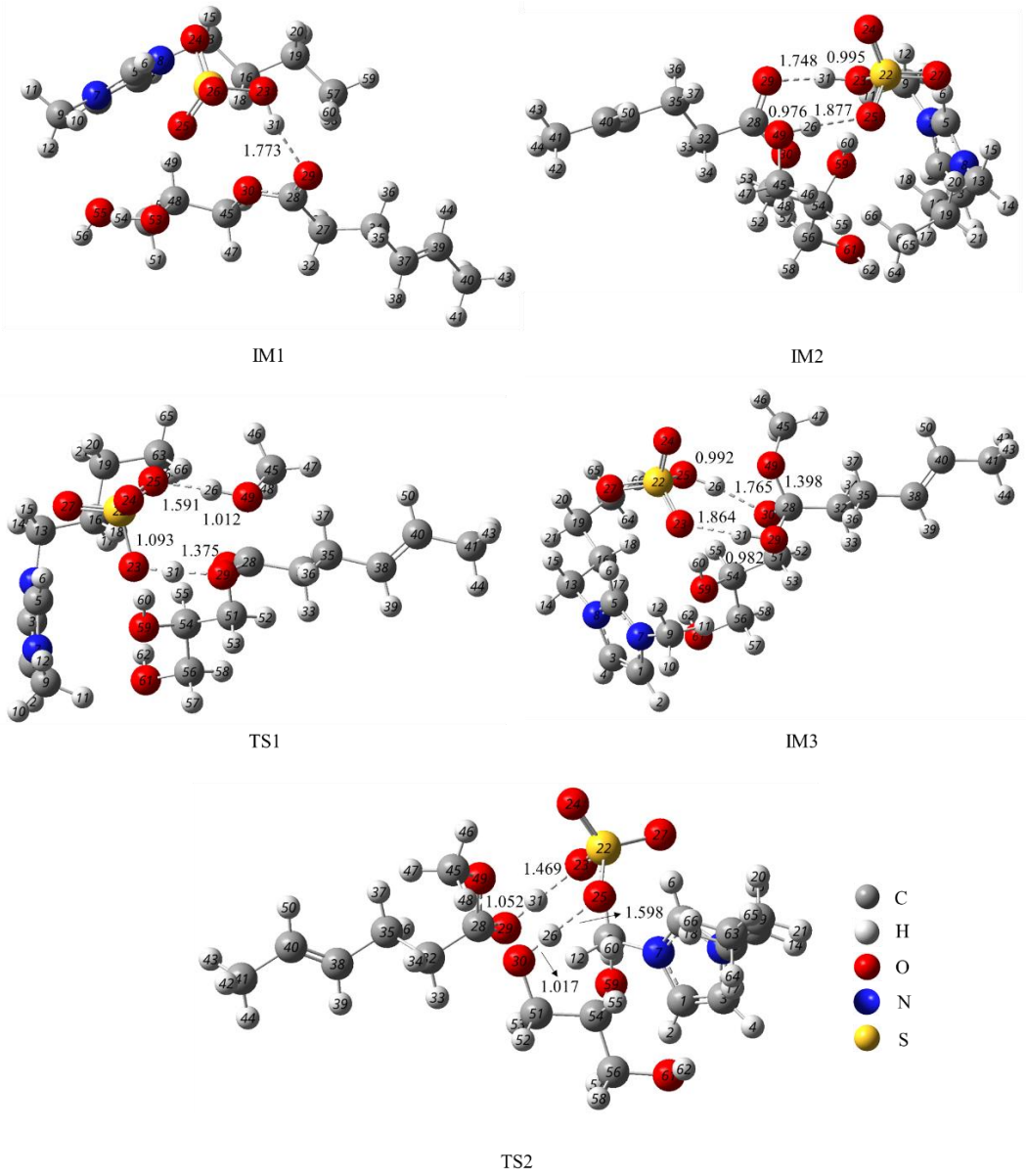

Fig. 8 IMs and TSs in transesterification catalyzed by [Bmim][HSO_4]

With the further movement of H31 from O31 to O29, and H26 from O49 to O25, the geometry changes to IM3. In IM3, the length of hydrogen bond between hydrogen atom H31 and oxygen atom O23 is 1.864 Å, and the bond order is 0.5. The length of bond between H31 and O29 is 0.982, and the bond order is 1.0. This shows the bond between H31 and O29 is strong, and the atom H31 has escaped the attraction of O23. Apart from this, the distance between hydrogen atom H26 and oxygen atom O49 increases to 2.475 Å, while the bond between H26 and O25 is 0.992 Å, and the bond order is 1.0. This demonstrates the hydrogen atom H26 has escaped the attraction of O49, and has formed a strong bond with O25. Besides, a hydrogen bond between H26 and O30 appears. The

length of bond between the two atoms is 1.765 Å, and the bond order is 0.5, which means the hydrogen bond is weak. At the same time, a bond between oxygen atom O49 and carbon atom C28 formed. The length of the bond is 1.398 Å, and the bond order is 1.0. This indicates the bond is strong enough, and the tetrahedral structure has established.

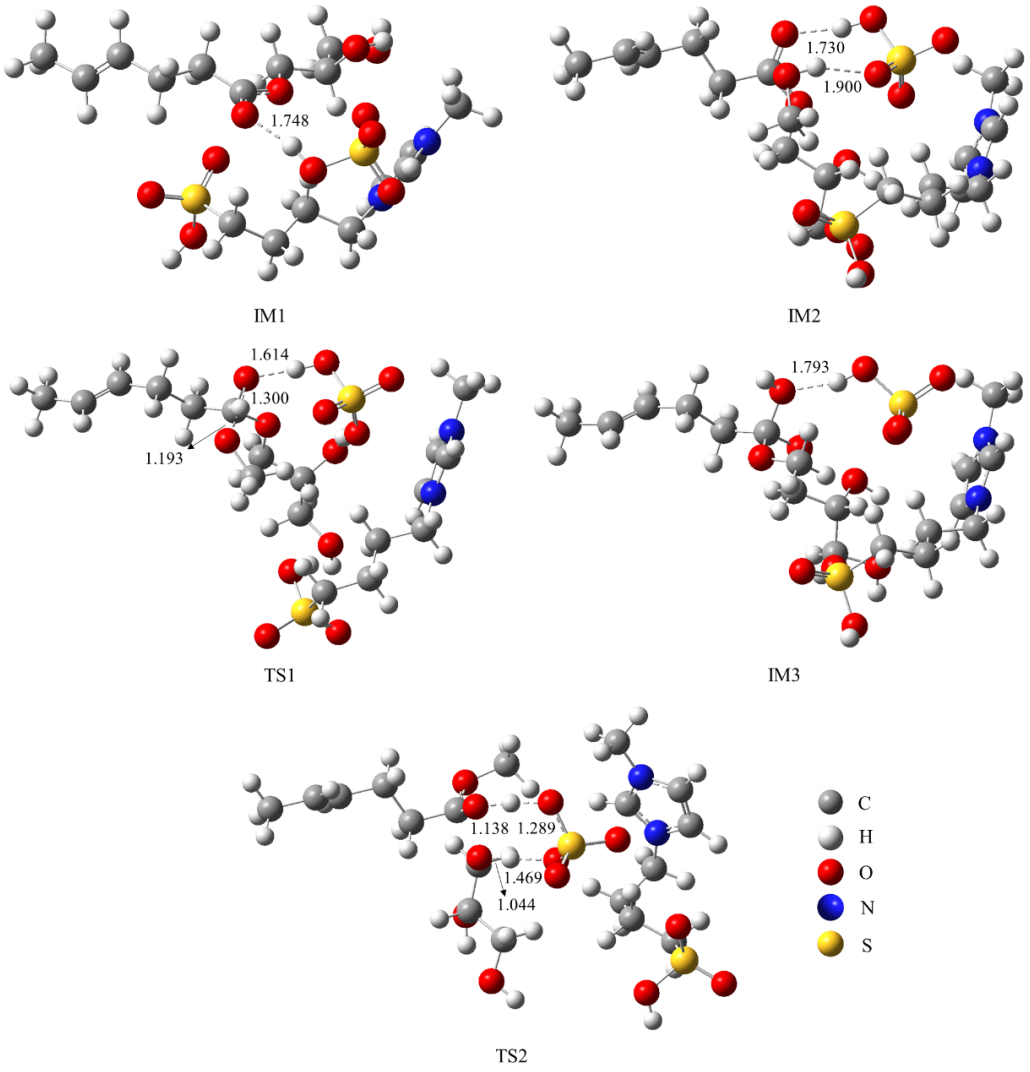

Fig. 9 IMs and TSs in transesterification catalyzed by [HSO_3-Bmim][HSO_4]

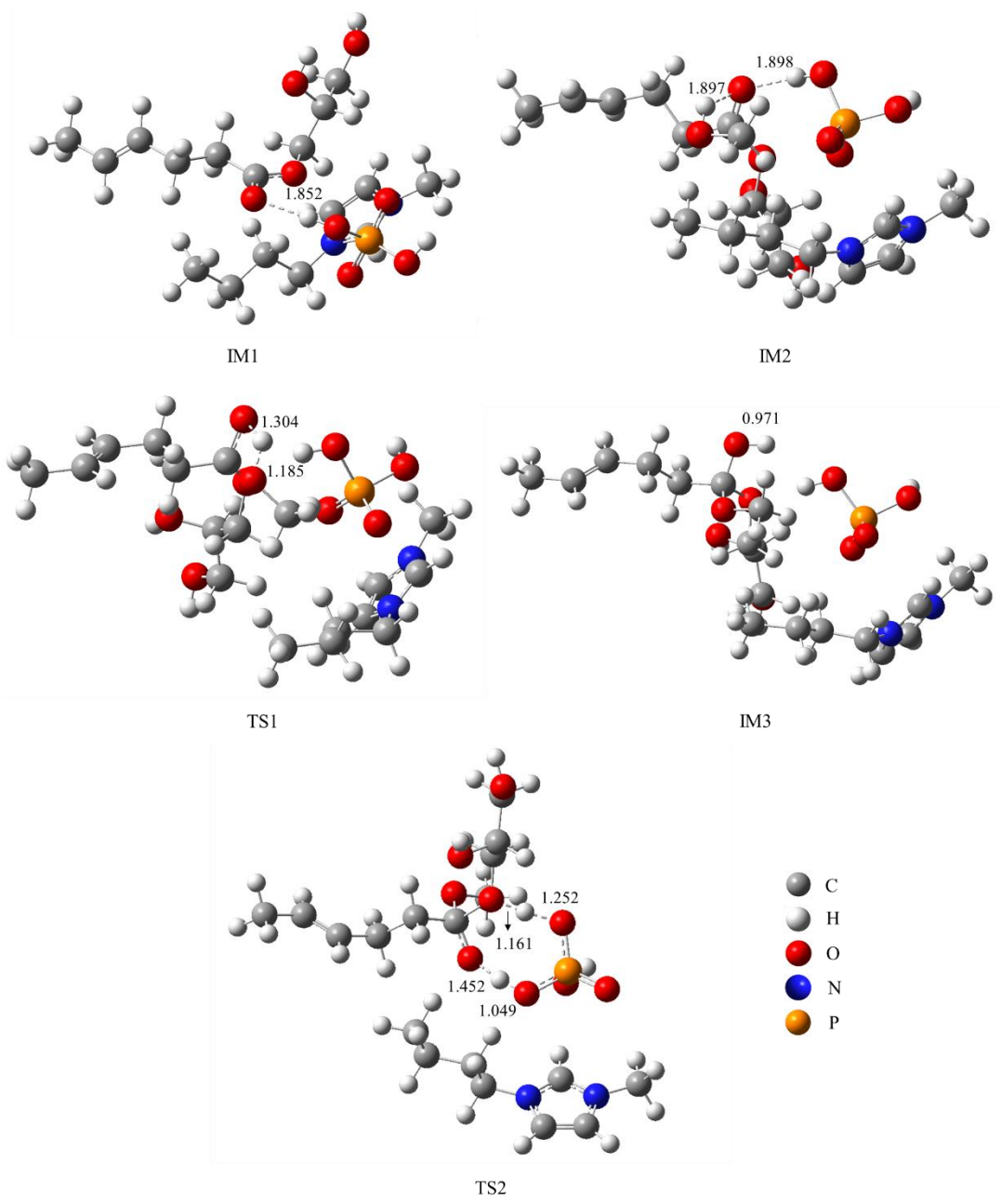

Fig. 10 IMs and TSs in transesterification catalyzed by [Bmim][H_2PO_4]

In TS2, the length of hydrogen bond between hydrogen atom H31 and oxygen O23 is 1.469 Å, and the length of hydrogen bond between hydrogen atom H31 and oxygen O29 is 1.052 Å. The bond orders of the two bonds are both 0.5. The results mean the bonds are not strong enough, and the hydrogen atom H31 has the trend of movement from O29 to O23. Apart from this, the length of hydrogen bond between the hydrogen atom H26 and oxygen atom O25 increases to 1.598 Å, and the length of hydrogen bond between the H26 and O30 decreases to 1.017 Å. The bond orders of the two bonds are both 0.5. This indicates the hydrogen atom H26 has the trend of movement from O25

to O30. Besides, the bond between O30 and C28 is broken. When the TS2 is optimized, a frequency of 202.46 icm^{-1} is obtained. The frequency is corresponding with vibration of the movement of H31 from O29 to O23, H26 from O25 to O30 and the departure of O30 from C28. The vibration is exactly the generation path of fatty acid methyl ester and glycerol.

Fig. 9 and Fig. 10 are the structures of IMs and TSs in transesterification catalyzed by [HSO_3-Bmim][HSO_4] and [Bmim][H_2PO_4], the reaction processes are similar with that catalyzed by [Bmim][HSO_4]. The imaginary frequency of TS1 and TS2 catalyzed by the three ionic liquids is shown in Table 3.

Table 3 Imaginary frequency of TS1 and TS2 catalyzed by the three ionic liquids (icm^{-1})

	[Bmim][HSO_4]	[HSO_3-Bmim][HSO_4]	[Bmim][H_2PO_4]
TS1	238.68	256.43	194.84
TS2	202.46	435.76	521.16

3.2.3 Analysis of Gibbs free energy

After all the geometry of IMs and TSs was optimized, the frequency of each IMs and TSs was calculated. Then the Gibbs free energy was obtained. The results are shown in Table 4.

Table 4 Gibbs free energy of each phase in transesterification catalyzed by three ionic liquids (Hartree)

	[Bmim][HSO_4]	[HSO_3-Bmim][HSO_4]	[Bmim][H_2PO_4]
R1	-653.19	-653.19	-653.19
R2	-115.67	-115.67	-115.67
IM1	-1775.92	-2399.69	-1719.83
IM2	-1891.58	-2515.35	-1835.50
TS1	-1891.56	-2515.33	-1835.48
IM3	-1891.59	-2515.36	-1835.51
TS2	-1891.57	-2515.32	-1835.49
Product	-424.21	-424.21	-424.21
$CH_2OHCHOHCH_2OH$	-344.65	-344.65	-344.65

R1: $CH_3CH=CHCH_2CH_2COOCHOHCH_2OH$

R2: CH_3OH

Product: $CH_3CH=CHCH_2CH_2COOCH_3$

Based on the calculation results in Table 4, use the same treatment as in section 3.1.3 for Gibbs free energy of each IMs and TSs. The calculation results are shown in Fig. 11.

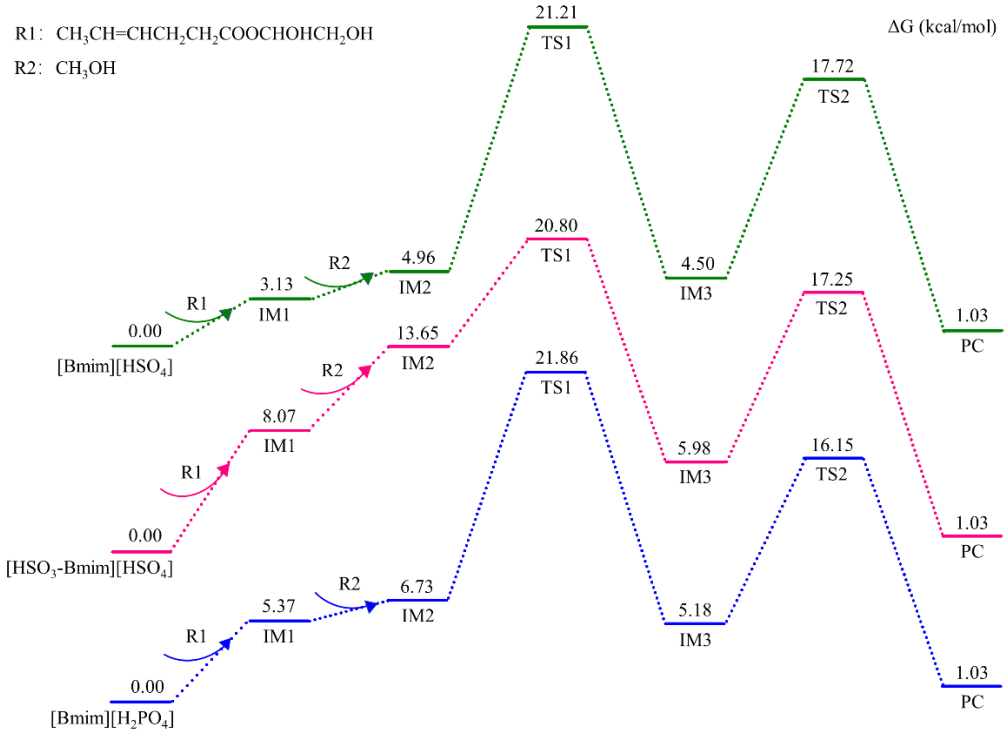

Fig. 11 Gibbs free energy in each phase of transesterification catalyzed by three ionic liquids

According to Murdoch[31], it is obvious that the processes of transesterification can be divided into two period, one is ionic liquid to IM3, and another is IM3 to PC. The two periods contain two energy barriers, one is ionic liquid to TS1 and another is IM3 to TS2. It can be easily found that the energy barrier of ionic liquid to TS1 is much higher than that of IM3 to TS2, so the process of ionic liquid to TS1 is the rate-limiting step. After calculation, the ΔG_{max} of transesterification catalyzed by $[Bmim][HSO_4]$, $[HSO_3$-$Bmim][HSO_4]$ and $[Bmim][H_2PO_4]$ are 21.21 kcal/mol, 20.80 kcal/mol and 21.86 kcal/mol, respectively. The results indicate that the ΔG_{max} of transesterification catalyzed by $[HSO_3$-$Bmim][HSO_4]$ is the lowest, and $[Bmim][H_2PO_4]$ is the highest. The calculation results reveals $[HSO_3$-$Bmim][HSO_4]$ and $[Bmim][H_2PO_4]$ has the best the worst catalytic effects in transesterification reactions. The DFT results consistent

with the experimental results and other DFT research[8, 32].

4.Conclusions

Based on DFT calculations, the catalytic mechanism of esterification and transesterification by acidic imidazolium ionic liquid [Bmim][HSO_4], [HSO_3-Bmim][HSO_4] and [Bmim][H_2PO_4] was discussed. The reaction pathways of transesterification and transesterification catalyzed by three acidic ionic liquids were proposed. Three intermediates and two transition states were found to be contained in both of the pathways. The intermediates and transition states in each reaction phase were optimized and verified by frequency calculations and intrinsic reaction coordinate (IRC) calculations. The Gibbs free energy of the intermediates and transition states in each reaction phase was then calculated. By analyzing the variation of Gibbs free energy along the reaction pathway, it was found that the esterification contained one period, and the rate-limiting step was IM2 to TS1. The transesterification contained two periods, and the rate-limiting step was ionic liquid to TS1. Based on the results above, the energy barrier of each reaction was obtained. It showed that the esterification reaction catalyzed by [Bmim][HSO_4] had the minimum energy barrier of 37.77 kcal/mol, and the reaction catalyzed by [Bmim][H_2PO_4] had the maximum energy barrier of 49.34 kcal/mol. The energy barrier results revealed [Bmim][HSO_4] had the best catalytic effect in esterification. As for transesterification reactions, the reaction catalyzed by [HSO_3-Bmim][HSO_4] had the minimum energy barrier of 20.80 kcal/mol, and the reaction catalyzed by [Bmim][H_2PO_4] had the maximum energy barrier of 21.86 kcal/mol, indicating [HSO_3-Bmim][HSO_4] had the best catalytic effect in transesterification. All the calculation conclusion were consistent with previous experimental results. On the other hand, the results also validate the correction of the proposed reaction pathways. The validated catalytic mechanism will provide a new idea for subsequent optimization of imidazolium ionic liquid structure to improve their catalytic efficiency in biodiesel production from oleaginous yeast.

Acknowledgments

396 The study (No. 2022-GH12) was supported by the International Joint Research Center
397 for Biomass Materials (Southwest Forestry University), the 111 Project (D21027) and
398 Open Project of Jiangsu Provincial Key Laboratory of Eco-Environmental Materials.
399

References:

[1] Akram F, Haq IU, Raja SI, Mir AS, Qureshi SS, Aqeel A, et al. Current trends in biodiesel production technologies and future progressions: A possible displacement of the petro-diesel. J Clean Prod. 2022;370.

[2] Kumar A, Singh VP, Srivastava A. Quality biodiesel via biotransesterification from inedible renewable sources. J Clean Prod. 2022;379.

[3] Shi Y, Zhou Y, Li Z, Cai Y, Li X, He Y, et al. Effect of temperature control conditions on DPF regeneration by nonthermal plasma. Chemosphere (Oxford). 2022;302:134787.

[4] Gao Z, Wu S, Luo J, Zhang B, Zhang H, Xiao R. Optimize the co-solvent for methanol in diesel with group of oxygen-containing reagents: Molecular structure and intermolecular forces analysis. Fuel Process Technol. 2021;222:106980.

[5] Wang G, Wang Y, Lv J, Wu Y, Jin L, Li Y, et al. Effect of red mud-based additives on the formation characteristics of tar and gas produced during coal pyrolysis. J Energy Inst. 2022;104:1-11.

[6] Li X, Fan Q, Wu Y, Lin X, Ma S, Li S, et al. Enhancing hydrodeoxygenation-isomerization of FAME over M-SAPO-11 in one-step process: Effect of in-situ isomorphic substitution of transition metals and synergy of PtxSny alloy. Chem Eng J. 2023;452:139528.

[7] Huang Y, Wang H, Zhang X, Zhang Q, Wang C, Ma L. CO2 pyrolysis kinetics and characteristics of lignin-rich hydrolysis residue produced from a tandem process of steam-stripping and acid hydrolysis. Fuel. 2022;316:123361.

[8] Chen Y, Long F, Huang Q, Wang K, Jiang J, Chen J, et al. Biodiesel production from Rhodosporidium toruloides by acidic ionic liquids catalyzed hydrothermal liquefaction. Bioresour Technol. 2022;364:128038.

[9] Wang F, Xu H, Yu S, Zhu H, Du Y, Zhang Z, et al. Fe-promoted Ni catalyst with extremely high loading and oxygen vacancy for lipid deoxygenation into green diesel. Renew Energ. 2022;197:40-9.

[10] Saini R, Hegde K, Brar SK, Vezina P. Advanced biofuel production and road to commercialization: An insight into bioconversion potential of Rhodosporidium sp. Biomass and Bioenergy. 2020;132:105439.

[11] Sutanto S, Zullaikah S, Tran-Nguyen PL, Ismadji S, Ju Y. Lipomyces starkeyi: Its current status as a potential oil producer. Fuel Process Technol. 2018;177:39-55.

[12] Chen Y, Nie X, Ye J, Wang Y, Chen J, Xu J. Biodiesel from Microorganisms: A Review. Energy Technol-Ger. 2021;9(10).

[13] Jin G, Zhang Y, Shen H, Yang X, Xie H, Zhao ZK. Fatty acid ethyl esters production in aqueous phase by the oleaginous yeast Rhodosporidium toruloides. Bioresource Technol. 2013;150:266-70.

[14] Chen Y, Huang Q, Ye J, Xu J, Chen J, Wang Y, et al. Study on hydrothermal liquefaction for cell disruption and lipid extraction from Rhodosporidium toruloides. Sustain Energ Fuels. 2021;5(23).

[15] Ong HC, Tiong YW, Goh BHH, Gan YY, Mofijur M, Fattah IMR, et al. Recent advances in biodiesel production from agricultural products and microalgae using ionic liquids: Opportunities and challenges. Energ Convers Manage. 2021;228:113647.

[16] Roman FF, Ribeiro AE, Queiroz A, Lenzi GG, Chaves ES, Brito P. Optimization and kinetic study of biodiesel production through esterification of oleic acid applying ionic liquids as catalysts. Fuel.

2019;239:1231-9.
[17] Sun S, Cheng X, Ma M, Liu Y, Wang G, Yu H, et al. High-efficient esterification of rosin and glycerol catalyzed by novel rare earth Lewis acidic ionic liquid: Reaction development and mechanistic study. J Taiwan Inst Chem E. 2021;127:1-6.
[18] Gao J, Zhu Y, Liu W, Jiang S, Zhang J, Ma W. Hydrogen Bonds in Disulfonic-Functionalized Acid Ionic Liquids for Efficient Biodiesel Synthesis. ACS Omega. 2020;5(21):12110-8.
[19] Hu S, Li Y, Lou W. Novel efficient procedure for biodiesel synthesis from waste oils with high acid value using 1-sulfobutyl-3-methylimidazolium hydrosulfate ionic liquid as the catalyst. Chinese J Chem Eng. 2017;25(10):1519-23.
[20] Seddon KR, Gilea MA, Rebelo LPN, Earle MJ, Esperança JMSS, Widegren JA, et al. The distillation and volatility of ionic liquids. Nature. 2006;439(7078):831-4.
[21] Wasserscheid P. Chemistry: volatile times for ionic liquids. Nature. 2006;439(7078):797.
[22] Da Silva ACH, Dall Oglio EL, de Sousa Jr. PT, Da Silva SC, Kuhnen CA. DFT study of the acid-catalyzed ethanolysis of butyric acid monoglyceride: Solvent effects. Fuel. 2014;119:1-5.
[23] Ma T, Shen Z, Li H, Li A, Feng Q, Sun Y, et al. Effect of H-Bonding on Brønsted Acid Ionic Liquids Catalyzed In Situ Transesterification of Wet Algae. Acs Sustain Chem Eng. 2020;8(11):4647-57.
[24] Li K, Yang Z, Zhao J, Lei J, Jia X, Mushrif SH, et al. Mechanistic and kinetic studies on biodiesel production catalyzed by an efficient pyridinium based ionic liquid. Green Chem. 2015;17(8):4271-80.
[25] Frisch MJ, Trucks GW, Schlegel HB, Scuseria GE, Robb MA, Cheeseman JR. Gaussian 16 A.03. Wallingford, CT2016.
[26] Chai JD, Head-Gordon M. Long-range corrected hybrid density functionals with damped atom-atom dispersion corrections. Phys Chem Chem Phys. 2008;10(44):6615-20.
[27] Grimme S, Ehrlich S, Goerigk L. Effect of the damping function in dispersion corrected density functional theory. J Comput Chem. 2011;32(7):1456-65.
[28] Fukui K. The path of chemical reactions - the IRC approach. Accounts Chem Res. 1981;14(12):363-8.
[29] Semichem I. GaussView 6.0.16.
[30] Clark JH, Farmer TJ, Macquarrie DJ, Sherwood J. Using metrics and sustainability considerations to evaluate the use of bio-based and non-renewable Brønsted acidic ionic liquids to catalyse Fischer esterification reactions. Sustainable chemical processes. 2013;1(1):1-23.
[31] Murdoch JR. What is the rate-limiting step of a multistep reaction? J Chem Educ. 1981;58(1):32.
[32] Limpanuparb T, Punyain K, Tantirungrotechai Y. A DFT investigation of methanolysis and hydrolysis of triacetin. Journal of Molecular Structure: THEOCHEM. 2010;955(1-3):23-32.